CONCRETE LIBRARY OF JSCE NO. 29, JUNE 1997

MATHEMATICAL MODELING FOR PERMEABLE BEHAVIOR OF HOMOGENEOUS MATERIAL AND ITS APPLICABILITY

(Translation from Proceeding of JSCE, No.526 / V-29, November 1995)

Hideki OSHITA

Tada-aki TANABE

An analytical model for water migration is applicable to porous permeable materials such as concrete and rock is constructed. Analysis of pore water pressure occurring in concrete is carried out, and then the applicability of the proposed model is demonstrated by comparison with experimental results. Further, the mechanisms for water migration, pore water pressure, effective stress and total stress are investigated and the effects of pore water pressure on the stress characteristics of concrete are estimated analytically, and it is then shown that water migration in concrete is very important.

Keywords: *water migration, mass conservation law, force equilibrium equation, homogeneous material, coefficient of permeability, pore water pressure, effective stress, total stress*

Hideki Oshita is an Assistant Professor in the Department of Civil Engineering at the National Defense Academy, Yokosuka, Japan. He obtained his Dr. Eng. from Nagoya University in 1995. His research interests relate to the characteristics of water migration in concrete and the deformation mechanism of composite structures. He is a member of the JSCE and JCI.

Tada-aki Tanabe is a Professor in the Department of Civil Engineering at Nagoya University, Nagoya, Japan. He obtained his Dr. Eng. from Tokyo University in 1971. His research interests include thermal stress behavior, characteristics of water migration, and constitutive equations for young and hardened concrete. He is a member of the JSCE, JCI, RILEM, and IYBSE.

1. INTRODUCTION

A recently focus of civil engineering is to utilize concrete structures such as deep underground structures and marine structures. In such structures, the main external forces are earth pressure and water pressure, and the characteristics of water migration in concrete must be clarified to secure the safety and durability in design. Water migration in concrete is a particularly important design factor in the rational design of waste disposal facilities, where the characteristics of water migration are important due to the difficulties of maintenance and repair once in service and to secure of durability in the long term. Though water migration is very important and there are many phenomenon that are related in same way with water migration in concrete, water migration is very important there are few studies which aside from those by these authors estimate water migration qualitatively or quantitatively, or which estimate the pore water pressure occurring in the infinitesimal pores in concrete experimentally.

The authors[1] have developed a cell which enables the pore water pressure arising in the pre-peak region of concrete due to the application of external load to be measured. They have carried our experiments measuring the pore water pressure under tri-axial displacement conditions and with pore water undrained. According to this experimental study, a high rate of pore water pressure compared with the loading stress occurs and the main factors affecting pore water pressure in the pre-peak region are volumetric contraction and water content. There is an inflection point in the relationship between stress and strain which indicates existence of the negative pore water pressure caused by the hydration reaction as the concrete specimen cures. The inflection point corresponds to an interfacial point below which pore water pressure is low and a gradual increase in stress occurs, while this strain point pore water pressure increases linearly and stress rises the loading stress. In past discussions stress-strain relations, only in the latter stage, i.e., above the corresponding strain. In the region of loner strain, the relation is closely related to autogeneous shrinkage problems. Thus studies on pore water pressure in concrete are very important. However, the applicable range of the experiments performed by the authors on pore water pressure in the pre-peak region is limited to that of the experimental parameters, i.e. the applicable range is very narrow. Hence, an analytical technique must be introduced to estimate water migration in concrete in detail.

In this study, we develop an analytical model for water migration which is applicable to porous permeable materials such as concrete and rock. The applicability of this model to the estimation of pore water pressure occurring in the pre-peak region of concrete is demonstrated by comparing analytical and experimental results. Moreover, a discussion of pore water pressure is given and the effects of pore water pressure on the mechanical characteristics of concrete are also discussed analytically. Further, a mechanism for the effects of pore water pressure on concrete strength is derived a the basis of the analytical results for a concrete specimens completely saturated and completely unsaturated with water. Experiments in the pre-peak region of concrete of which condition is fixed of lateral displacement and perfectly undrained of pore water, were carried out. The experimental parameters were loading age, water curing period, age at pre-loading stress, and ratio of pre-loading stress to the uni-axial compressive strength (called damage).

2. Modeling Concrete as a Homogeneous Porous Permeable Material

The modeling of concrete as a homogeneous porous permeable material such that CSH gel particles and the aggregate particles are considered to be elastic and then the mixed materials may allow shear deformation by changing the relative location of each particles, hence it may be reasonable to assume that it is a hardening visco-plastic material with reducing pore volumes fully saturated or partially saturated with water with increasing age. Since concrete is modeled as a two-phase porous material consisting of solid and liquid in the model, the mass conservation law and the force equilibrium equation must be satisfied, as shown in Fig.1. Hence, the mass conservation law and force equilibrium equation must first be formulated independently before finally formulating then into a a governing equation which can estimate the characteristics of water migration in concrete in detail. In the following formulations, the pore water pressure is assumed to represent the sum of pore pressures occurring in the liquid and gas phases.

2.1 Formulation of Mass Conservation Law Considering Volumetric Contraction by Hydration

The flow velocity of pore water[2] is considered to be linearly dependent on the gradient of the Gibb s free energy

G.

$$v_i = -K_{ij}\nabla_j G \tag{1}$$

Where K_{ij} is the coefficient matrix of permeability and G in water-saturated and non-saturated conditions is

$$G = (\gamma_w z + p)/\gamma_w \tag{2}$$
$$G = \frac{RT}{M}\ln(H) + G_{sat}$$

where γ_w is the specific gravity of water and z is the vertical coordinate. R, H, and M are the gas constant, relative humidity, and mole cular weight of water, and G_{sat} is the Gibb s Free Energy when saturated with water.

From the mass conservation law, the amount of fluid accumulated in a controlled unit volume is equal to the difference between the inflow and outflow to this volume. The following contributions to the amount of fluid accumulated in this volume exist:

a) Total strain change

$$\rho_w S_w \frac{\partial \varepsilon_V}{\partial t} = \rho_w S_w m_{ij}^T \frac{\partial \bar{\varepsilon}_{ij}}{\partial t} \tag{3}$$

b) Change in volume of particles caused by changes in hydrostatic pressure

$$\rho_w S_w (1-\xi) m_{ij}^T D_{S\ ijkl}^{ep\ -1} m_{kl} \frac{\partial p}{\partial t} \tag{4}$$

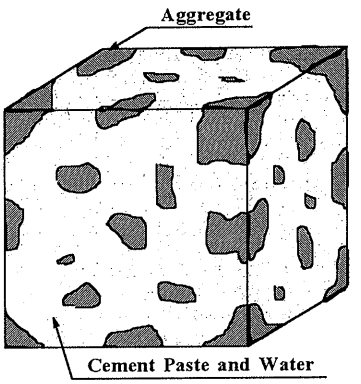

(a) Concrete as Two Phase Porous Material

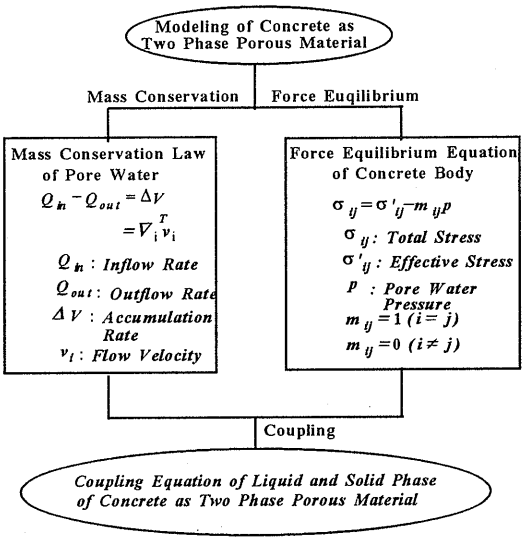

(b) Flowchart of Modeling of Concrete

Fig.1 Concrete as Homogeneous Material

c) Change in degree of saturation with water

$$\xi \rho_w \frac{\partial S_w}{\partial t} \tag{5}$$

d) Change in liquid and gas volumes caused by changes in hydrostatic pressure

$$\xi \rho_w S_w \frac{1}{K_f} \frac{\partial p}{\partial t} \tag{6}$$

e) Change in liquid and gas volumes caused by temperature

$$-3\xi\mu \frac{\partial T}{\partial t} \tag{7}$$

f) Change in liquid and gas volumes caused by creep

$$-\rho_W S_W \xi m_{ij}^T \frac{\partial \varepsilon_{ij}^{cr}}{\partial t} \tag{8}$$

where ε_{ij}^{cr} is the creep strain.

g) Change in particle size caused by the effective stress

$$-\rho_w S_w m_{ij}^T D_{S\ ijkl}^{ep\,-1} \frac{\partial \sigma_{kl}'}{\partial t} \tag{9}$$

where ρ_w is the density, S_w is the degree of saturation, K_f is the bulk modulus of the liquid and gas phases, μ is the coefficient of thermal expansion of liquid and gas phases and ξ is the porosity which depends on the hydration ratio of the cement. The matrix D_{Sijkl}^{ep} is the elasto-plastic stiffness matrix of the solid phase and the vector $m_{ij} = [1 \ \ 1 \ \ 1 \ \ 0 \ \ 0 \ \ 0]^T$.

h) Volumetric contraction caused by hydration

$$\rho_w S_w \frac{\eta \gamma_p}{\rho_w} \frac{dC_H}{dt} \tag{10}$$

where η is the ratio of gel pore volume due to hydration to initial cement volume, γ_p is the water-cement ratio at complete hydration, and C_H is the hydrated cement weight per unit cement volume. Eq.(10) indicates the pore water weight change caused by hydration of cement, hence the pore water weight change per unit concrete volume can be written as follows.

$$\rho_w S_w \frac{\eta \gamma_p}{\rho_w} \frac{dC_H}{dt} \frac{V_c}{V} \tag{11}$$

where V, V_c are the volume of concrete and cement paste per unit controlled volume.
In this study, the hydration process of cement paste proposed by Kawasumi et al[3]. is introduced. Assuming the rate of hydration is controlled by the amount of unhydrated cement and water, the hydration process can be written as follows.

$$\frac{dC_H}{dt} = k_0 (1 - n_0) t^{-n_0} (W - \gamma_p C_H)(C - C_H) \tag{12}$$

where C, W, and t are the initial cement weight, initial water weight, and age, respectively. The solution ot differential Eq.(12) is obtained in explicit form as follows.

When $W / C \neq \gamma_P$,

$$C_H = \frac{1 - \exp\left[\left(\gamma_p C - W\right) k_0 t^{1-n_0}\right]}{1 - \gamma_p C/W \exp\left[\left(\gamma_p C - W\right) k_0 t^{1-n_0}\right]} \times C \tag{13}$$

When $W / C = \gamma_P$,

$$C_H = \frac{\gamma_p k_0 t^{1-n_0}}{1 + \gamma_p k_0 t^{1-n_0}}$$

The factors γ_p and η are determined according to the study by W.Czernin[4] and are known to take values 1.25 $\sim$ 0.38.

By equating the total accumulation of weight to the sum of the terms a)~h), the mass conservation law can be written as follows.

$$\rho_w S_w[\xi m_{ij}^T \frac{\partial \varepsilon_{ij}}{\partial t} + \frac{\xi}{K_f}\frac{\partial p}{\partial t} + 3\{(1-\xi)\alpha - \xi\mu\}\frac{\partial T}{\partial t} +$$
$$\frac{V_C}{V}\frac{\eta\gamma_p}{\rho_W}\frac{\partial C_H}{\partial t} + \{(1-\xi)\frac{V_C}{V} - \xi\} m_{ij}^T \frac{\partial \varepsilon_{ij}^{cr}}{\partial t}] + \tag{14}$$
$$\xi\rho_w \frac{\partial S_W}{\partial t} - \rho_w \nabla_i^T \frac{K_{ij}}{\rho_w}\nabla_j(\rho_w z + p) - q = 0$$

where q is the spring flow from the unit controlled volume. Assuming the degree of saturation to be constant with age, the sixth term in the left-hand side of Eq.(14) reduces to zero.

$$\xi m_{ij}^T \frac{\partial \varepsilon_{ij}}{\partial t} + \frac{\xi}{K_f}\frac{\partial p}{\partial t} + 3\{(1-\xi)\alpha - \xi\mu\}\frac{\partial T}{\partial t} +$$
$$\frac{V_C}{V}\frac{\eta\gamma_p}{\rho_W}\frac{\partial C_H}{\partial t} + \{(1-\xi)\frac{V_C}{V} - \xi\} m_{ij}^T \frac{\partial \varepsilon_{ij}^{cr}}{\partial t}$$
$$- \nabla_i^T \frac{K_{ij}}{\rho_w}\nabla_j(\rho_w z + p) - \frac{q}{\rho_w} = 0 \tag{15}$$

Applying the Method of Weight Residuals (MWR), Eq.(15) becomes.

$$-H\cdot\bar{p} - L_i^T \frac{d\bar{u}_i}{dt} - S\frac{d\bar{p}}{dt}$$
$$-W\frac{d\bar{T}}{dt} - \frac{dg_p}{dt} - \frac{df_p^{cr}}{dt} + f_p^{ext} = 0 \tag{16}$$

where the vectors $\bar{u}_i$ and $\bar{p}$ are the nodal displacement vector and nodal water pressure, respectively. The matrices H, L^T, S, W represent the effect of pore water pressure on the compressibility of the liquid phase, the effect of displacement on the compressibility of the solid phase, the effect of pore water pressure on the compressibility of the solid phase, and the effect of temperature while vectors g_p, f_p^{cr}, f_p^{ext} are the volumetric contraction due to hydration of liquid phase, the effect of creep, and the flow rate. These are there were written as follows.

$$H = \int_\Omega (\nabla_i \bar{N})^T \frac{K_{ij}}{\rho_w}\nabla_j \bar{N}\, d\Omega, S = \int_\Omega \bar{N}^T \frac{\xi}{k_f}\bar{N}\, d\Omega$$
$$L_i^T = \xi\int_\Omega \bar{N}^T m_{ij}^T B_j\, d\Omega$$
$$W = \int_\Omega \bar{N}^T\{3(1-\xi)\alpha - 3\xi\mu\}\bar{N}\, d\Omega$$
$$f_p^{cr} = \int_\Omega \{(1-\xi)\frac{V_C}{V} - \xi\} m_{ij}^T \varepsilon^{cr}{}_{ij}\, d\Omega$$
$$f_p^{ext} = \int_\Omega \bar{N}^T q/\rho_w\, d\Omega - \int_\Omega (\nabla_i \bar{N})^T \frac{K_{ij}}{\rho_w}\nabla_j \rho_w z\, d\Omega + \int_\Gamma \bar{N}^T(\{v\}^T\cdot n)\, d\Gamma$$

$$g_P = \int_{\Omega} \overline{N}^T \frac{V_C}{V} \frac{\eta \gamma_p}{\rho_W} C_H \, d\Omega$$

2.2 Formulation of Force Equilibrium Equation

With the presence of pore water pressure p, the relationship between total stress σ_{ij} and effective stress $\sigma_{ij}^{'}$ can be written as follows, where the sign of stress Is positive for tensile stress and compressive stress is positive for pressure.

$$\sigma_{ij} = \sigma_{ij}^{'} - m_{ij} \cdot p \tag{17}$$

The effective stress in Eq.(17) which applies to the solid phase of concrete can be written incrementally as follows.

$$d\sigma_{ij}^{'} = D_{S\ ijkl}^{ep} \left(d\varepsilon_{ij}^{t} - d\varepsilon_{ij}^{pr} - d\varepsilon_{ij}^{hyd} - d\varepsilon_{ij}^{cr} \right) \tag{18}$$

where

$$d\varepsilon_{ij}^{t} = \frac{V_A}{V} d\varepsilon_{Aij}^{t} + \frac{V_C}{V} d\varepsilon_{Cij}^{t} \tag{19}$$

$$d\varepsilon_{ij}^{pr} = \frac{V_A}{V} d\varepsilon_{A\ ij}^{pr} + \frac{V_C}{V} d\varepsilon_{C\ ij}^{pr} \tag{20}$$

$$d\varepsilon_{ij}^{hyd} = \frac{1}{3} \frac{V_C}{V} \frac{\eta \gamma_p}{\rho_W} \frac{dC_H}{dt} m_{ij} \tag{21}$$

$$\varepsilon_{ij}^{cr} = a_0 \times \left[1 - \exp\left\{ b_0 \times (t_0 - t_0')^{c_0} \right\} \right] \tag{22}$$

where $d\varepsilon_{ij}^{t}$, $d\varepsilon_{ij}^{pr}$, $d\varepsilon_{ij}^{hyd}$, and $d\varepsilon_{ij}^{cr}$ are the incremental total strain, incremental strain of the solid phase due to pore water pressure, incremental volumetric contraction strain, and incremental creep strain, respectively. The subscripts A and C in these equations indicate aggregate and cement paste, respectively. Further, t_0 and t_0' are the age and loading age in days, and the a_0, b_0, and c_0 are material constants. The reason for incorporating the creep strain is explained as follows. In pore water pressure experiments[1], the strain (about $1000\,\mu$) corresponding to the inflection point at the age of 3 days is larger than that (about $500\,\mu$) at 7 days and hence it seems that the initial stress caused by the volumetric contraction due to hydration is relaxed due to the creep phenomenon.

Using the principle of virtual work and adopting the appropriate shape functions, The force equilibrium can be written as in differential form.

$$K_{T\,ij} \frac{d\overline{u}_j}{dt} - L_j \frac{d\overline{p}}{dt} - A_j \frac{d\overline{T}}{dt} - \frac{d\overline{f}_j}{dt} = 0 \tag{23}$$

where the matrices $K_{T\,ij}$, L_i ,and A_i are the tangential stiffness matrix, the effect of pore water pressure on the compressibility of the solid phase, and the effect of temperature, respectively. The vector $d\overline{f}_i$ is the incremental external force considering the effect of volumetric contraction and creep. These matrices and vectors can be defined as follows.

$$K_{Tij} = (1-\xi)\int_{\Omega} B_k{}^T D_S^{ep}{}_{ijkl} B_l \, d\Omega$$

$$L_i = \xi \int_{\Omega} B_j{}^T m_{ij} \overline{N} \, d\Omega$$

$$A_i = (1-\xi)\int_{\Omega} B_j{}^T D_S^{ep}{}_{ijkl} m_{kl} \, \alpha \overline{N} \, d\Omega$$

$$\bar{f}_i = \int_{\Omega} N^T b_i \, d\Omega + \int_{\Gamma} N^T t_i \, d\Gamma + (1-\xi)\frac{1}{3}\frac{V_C}{V}\frac{\eta \gamma_p}{\rho_w}\frac{C}{\rho_C}$$
$$C_H \int_{\Omega} B_j{}^T D_S^{ep}{}_{ijkl} m_{kl} \overline{N} \, d\Omega + (1-\xi)\frac{V_C}{V}\int_{\Omega} B_j{}^T D_S^{ep}{}_{ijkl} \varepsilon_{kl}^{cr} \, d\Omega$$

where α is the coefficient of thermal expansion of the solid phase and the vectors b_i, t_i are the body force and surface traction vector, respectively.

2.3 Governing Equation of Two-Phase Porous Material

The coupled mass conservation law and equilibrium equation can be written in matrix form as follows.

$$\begin{bmatrix} 0 & 0 \\ 0 & -H \end{bmatrix} \begin{Bmatrix} \{\overline{u}\} \\ \{\overline{p}\} \end{Bmatrix} + \begin{bmatrix} K_T & -L \\ -L^T & -S \end{bmatrix} \begin{Bmatrix} \dfrac{d\{\overline{u}\}}{dt} \\ \dfrac{d\{\overline{p}\}}{dt} \end{Bmatrix} = \begin{Bmatrix} \dfrac{d\{\bar{f}\}}{dt} + A\dfrac{d\{\overline{T}\}}{dt} \\ W\dfrac{d\{\overline{T}\}}{dt} + \dfrac{d\left\{f_p^{creep}\right\}}{dt} - \left\{f_p^{ext}\right\} + \dfrac{d\{g_P\}}{dt} \end{Bmatrix} \tag{24}$$

Finally, denoting the nodal displacement and pore water pressure in incremental form, Eq.(24) is transformed into the following equation:

$$\begin{bmatrix} K_T & -L \\ -L^T & -S - \Delta t_n H \end{bmatrix} \begin{Bmatrix} \Delta \overline{u}_n \\ \Delta \overline{p}_n \end{Bmatrix} = \begin{Bmatrix} \Delta \bar{f}_n + A\Delta \overline{T}_n \\ W\Delta \overline{T}_n - f_{pn}^{ext}\,\Delta t_n + \Delta f_{pn}^{creep} + \Delta g_{Pn} + \Delta t_n H \overline{p}_{n-1} \end{Bmatrix} \tag{25}$$

where the subscripts n and $n-1$ are the present step and the previous step number respectively.

$$\Delta \overline{u}_n = \overline{u}_n - \overline{u}_{n-1}, \Delta \overline{p}_n = \overline{p}_n - \overline{p}_{n-1}, \Delta \overline{T}_n = \overline{T}_n - \overline{T}_{n-1}$$
$$\Delta \bar{f}_n = \bar{f}_n - \bar{f}_{n-1}, \Delta g_{pn} = g_p(t_n) - g_p(t_{n-1})$$
$$\Delta f_{pn}^{creep} = f_p^{creep}(t_n) - f_p^{creep}(t_{n-1}), t_n = t_{n-1} + \Delta t$$

By solving these simultaneous equations in which the nodal displacement and pore water pressure are unknown, the characteristics of water migration in concrete as a homogeneous material can be obtained analytically. In actual analysis, Eq.(26) can be solved by substituting the boundary conditions and initial conditions.

3. DETERMINATION OF MATERIAL PARAMETERS FOR ANALYSIS

The proposed model was developed for application to porous materials such as concrete and rock. However, an examination of its applicability must be carried out by comparing it with experimental results and hence in this study the proposed model was applied to the concrete at early ages[1] to estimate the applicability of the proposed model. To use the developed analytical theory, a concrete specimen must be modeled and material parameters such as compressive strength, Young s modulus, permeability, cohesion, and internal friction angle in the plastic region must be determined. However, in analyzing the concrete at early ages, rapid changes in material properties with age must be taken into consideration due to the rapid progress of hydration. This means that, in the analysis, the stress state in the pores formed by hydration during curing must be taken into consideration[1]. Negative pore water pressure may arise in the voids formed by hydration, i.e., inflection points. This inflection point corresponds to an interfacial point of strain below which la pore water pressure and a gradual increase in stress occur, while at higher strains pore water pressure rises linearly along with stress.

3.1 Modeling of Concrete Specimen

The analytical model was one eighth of a prismatic section which was replaced such that the cross section is equal to that of the concrete specimen with the cylindrical type used in experiments of which diameter is 10 cm and the height is 20 cm, as shown in Fig.2. Further, all of elements were uncracked elements due to the experiments which is corresponding to the pre-peak region of concrete, i.e. one-dimensional consolidation phenomenon.

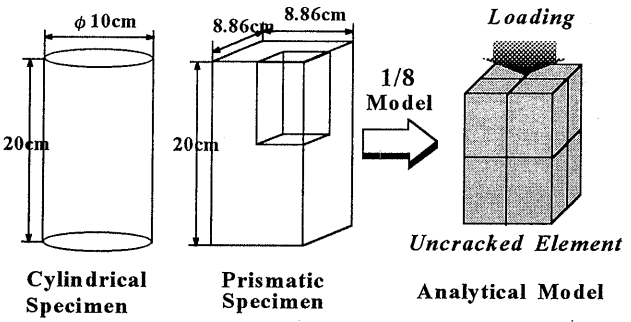

Fig. 2 Analytical Model of Concrete Specimen

3.2 Mechanical Characteristics of Concrete

The values of material parameters such as compressive strength and Young s modulus must be determined at each analytical steps to perform the analysis. In general, it is said that the general tendency is not lost even if compressive strength and Young s modulus are expressed as functions of maturity; these properties are expressed in terns of maturity in Figs.3 and 4. The mix proportion is such that the water-cement ratio = 0.60, cement content = 377 kg / m^3, and water content = 226 kg / m^3.

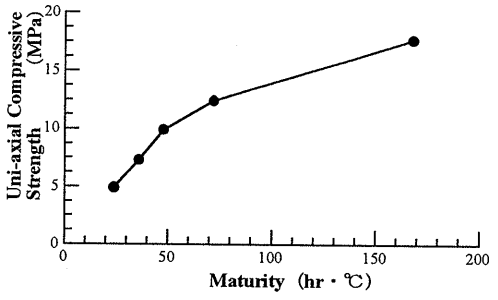

Fig. 3 Uni-Axial Compressive Strength

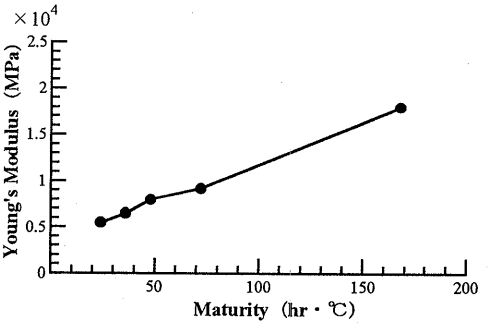

Fig. 4. Young's Modulus

3.3 Permeability of Concrete

J.Murata[5] performed permeability experiments an hardened concrete and reported a the relationship between permeability and water-cement ratio with maximum aggregate size as a parameter, as shown in Fig.5. Since

J.Murata did not report any results for early-age concrete, an extrapolation is made on the basis of the study performed by T.C.Powers[6], who proposed the relationship between age and permeability shown in Fig.6. These results are for concrete with a water-cement ratio of 0.70, but in this study it is assumed that this relation for reduction In permeability with age is constant for all mix proportions.

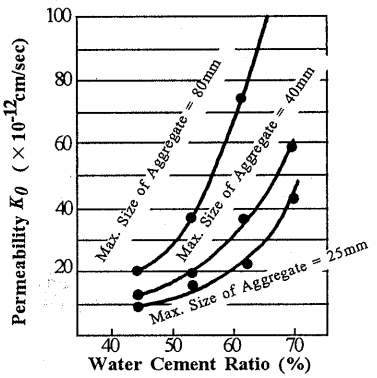

Fig. 5 Permeability Test[5]

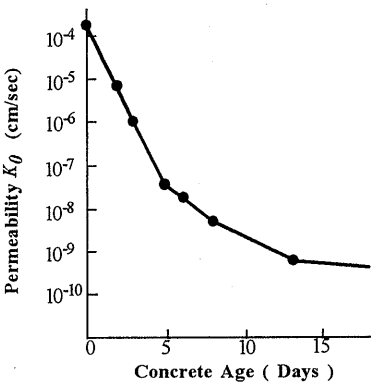

Fig. 6 Permeability Test[6]

3.4 Bulk Modulus of Liquid and Gas Phases

In general, concrete is an unsaturated material, but it is reported[1] that it becomes nearly saturated when an external load is applied to concrete cured in water due to the reduction in pore water pressure resulting from hydration and due to the reduction in pore volume caused by the external load. Hence, in this study, the water-cured concrete specimen is assumed to be saturated with water and the bulk modulus of the liquid and gas phases is taken to be 2,200 MPa, the value for water. If the concrete is near saturation, the presence of air pressure can be ignored compared with the water pressure due to the great difference in bulk modulus of the liquid and gas phases. On the other hand, for the specimen cured in air, it is reported[1] that even though the pore volume is reduced by the external load, It remains unsaturated due to the lack of water penetration into the specimen. In the analysis of the unsaturated concrete specimen, Therefore, the developed model can be applied If the bulk modulus is reduced, but this reduction can not be fixed arbitrarily Since bulk modulus changes considerably with the liquid-gas mix. Hence, for the unsaturated concrete specimen, the same value as for the saturated specimen, is used: 2200 MPa. As a result, it may be seen that the range of applicability of the developed model can be clarified and water migration in unsaturated concrete can be predicted by comparing the experimental results and analytical results assuming saturation of the concrete specimen.

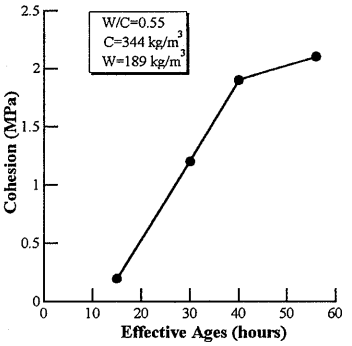

Fig. 7 Initial Cohesion

3.5 Cohesion and Internal Friction Angle in Plastic Region

A failure surface of Drucker-Prager type[7] is introduced as a plasticity model and hence material parameters such as cohesion and internal friction angle must be determined. Tri-axial compressive tests were performed on a cylindrical cement paste specimen having a diameter of 5 cm, a height of 10 cm, and a water cement ratio of 0.55 at the age of 0.5, 1.0, 1.5, and 2.0 days[8]. Then the relationships between cohesion, internal friction angle, and effective age were obtained, as shown in Figs.7 and 8. The experimental results obtained for cohesion, which increases with the effective age (maturity) are reasonable and it can be seen that the experimental cohesion is are quarter of the uni-axial compressive strength. The experimental results obtained for internal friction angle do not vary with the time and it can be seen that the internal friction angle falls in the range 27° to 31° . Though we can not generalize the applicability of these

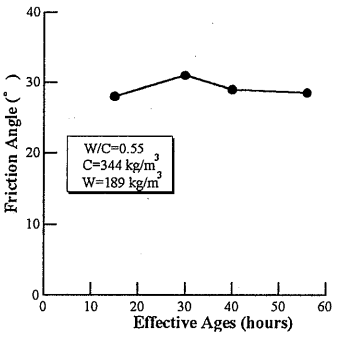

Fig. 8 Initial Internal Friction Angle

values to other mix proportions, the tendency itself may be generalized. In the analysis, uni-axial compressive strength is used to fix the value of cohesion and then the cohesion and internal friction angle vary with the degree of damage. The initial cohesion is are quarter of the uni-axial compressive strength and the initial internal friction angle is 29° .

4. INITIAL STRESS STATE IN CONCRETE DURING CURING

The hydration product CSH gel forms rapidly and generates pores of various sizes varying from tens of Å to μ m. The initial distribution of pore size is determined mainly by the cement particle distribution as well as aggregate particle distribution at mixing. It is said that the around quarter of gel water volume decreases compared with the initial volume and this phenomenon is well-known as Contraction by Hydration .

In the pore water pressure experiments, a gradual increase in total stress after loading occurs. In the region of strain below the inflection point, low pore water pressure and a gradual increase in stress occur. On the other hand, in the region of higher strain, the pore water pressure and stress rise linearly with increasing loading stress. The inflection point demonstrates the existence of negative pore water pressure caused by the volumetric contraction resulting from hydration. Though it seems that other factors also influence the initial stress state of pores, the volumetric contraction due to hydration is the main factor affecting the initial stress state in this study. In this section, the initial stress state due to hydration is estimated analytically using the material parameters obtained in the previous section. Moreover, the representative example effected of the initial stress state is a thermal stress problem and the effect of initial stress state on the thermal stress is discussed through a comparison of the results obtained by the developed model and by conventional thermal stress analysis which ignores the initial stress state.

4.1 Pore Water Pressure and Total Stress

To estimate the initial stress state in concrete resulting from the volumetric contraction due to hydration, the boundary conditions and material parameters representing the hydration rate of cement paste must be determined except for the material parameters given in the previous chapter. The boundary conditions were taken to be uni-axial stress conditions for displacement in pore water undrained. The material parameters k_0, n_0 were given the values 6.219×10^{-4} and 8.928×10^{-2} so as to make the hydration ratio at the age of 5 days about 50% of complete hydration.

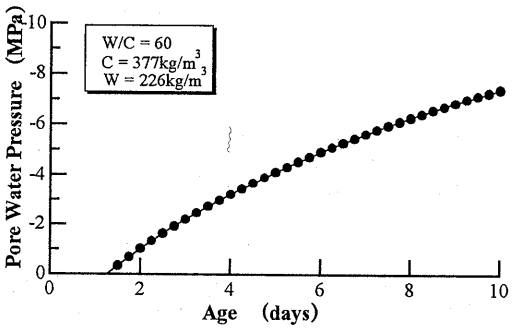

Fig. 9 Initial Pore Water Pressure

The analytical results are shown in Figs.9 and 10, which show the relationship between pore water pressure and age, and effective stress and age, respectively. As shown in Fig.8, a parabolic increase in negative pore water pressure (tension) occurs with age, i.e., with the progress of hydration. At ages 3 and 7 days Its value was 2.2 and 5.7 MPa, respectively. On the other hand, as shown in Fig.9, a parabolic increase in compressive effective stress occurs with the same absolute values as pore water pressure when application of no external load is applied One of the reasons for this, can be explained as follows. It is well-known that the absolute volume of concrete decreases with the degree of hydration and that, after the appearance of strength in the solid phase, minute voids are formed in the concrete due to the resistance of the solid phase to volumetric contraction. Hence, the compressive

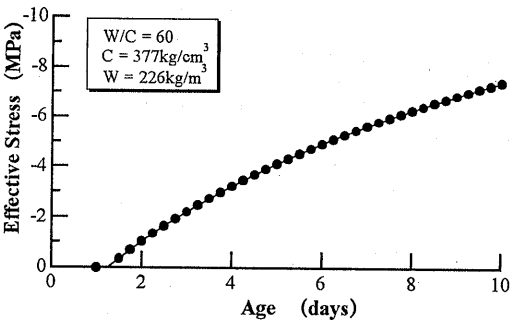

Fig. 10 Initial Effective Stress

stress arises in the solid phase which resists volumetric contraction, while an equivalent tensile stress occurs for minute voids. In the practice, both water and gas are present in the voids and hence the analytical condition in which the voids were saturated with water differs from the actual condition. However, most of the initial stress due to negative pressure arises from the water due to the difference in bulk modulus between water and gas. It should be noted that the negative increment in pore water pressure caused by hydration is greater as the degree of hydration rises, such as in early-age concrete. Further, it is clear that the initial stress state has a great influence on problems such as autogeneous shrinkage[9]. However, though this quantitative estimation of initial stress state has been rationally determined in an analytical sense, the applicability of the analytical results can not be verified due to a lack of experimental results and an experimental method of measuring initial stress state. There is thus an immediate need to establish an experimental method for determining the applicability of these analytical results. In the following analysis, the value of initial stress state obtained by the analysis is used as a crude approximation.

4.2 Effect of Initial Stress State on Thermal Stress

The most representative example which was greatly influenced by the initial stress state is a thermal stress problem. It should be noted that in conventional thermal stress analysis, the initial stress state shown in Figs.9 and 10 is not taken into consideration. In this section, the difference in results obtained by thermal stress analysis taking into account the initial stress state, i.e., the developed model is not, estimated. Further, the effects of pore water pressure on thermal stress are estimated. The analytical model is the simplest one-dimensional thermal stress state having a fixed displacement in the axial (vertical) direction, as shown in Fig.11(a). As regards deformational behavior with in changes concrete temperature, the solid and liquid phases expand as concrete temperature rises, and conversely contract as concrete temperature falls in the direction of the solid arrow shown in Figs.11(b) and 11(c). On the other hand, regarding the deformational behavior due to initial stress state, the solid phase expands and the liquid phase contracts in the direction of the dotted arrows and there is no relation to changes in concrete temperature. These deformational behaviors are assumed to apply uniformly in each phase.

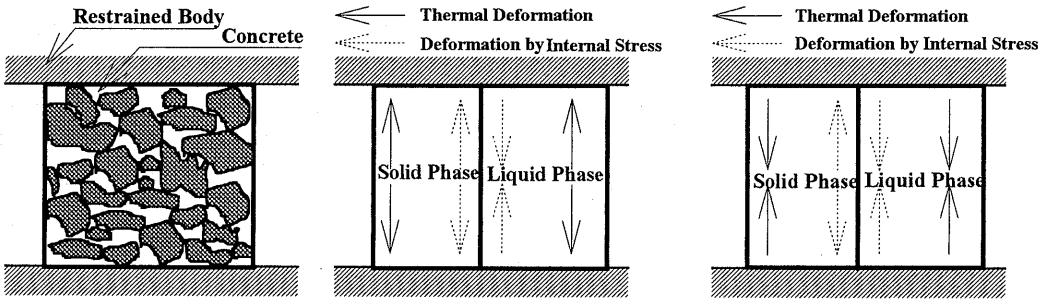

(a) One Dimensional Model **(b) Deformational Behavior (Rising of Concrete Temp.)** **(c) Deformational Behavior (Falling of Concrete Temp.)**

Fig. 11 Thermal Deformational Behavior

First, the effects of initial stress state and pore water pressure caused by thermal force on thermal stress behavior, ignoring the creep effect, was estimated using the parameters shown in Table.1. During the rise in concrete temperature, in the solid phase underwent expansive deformation as a result of both initial stress state and temperature, and hence a compressive effective stress of -2.5 MPa occurred as the sum of the initial compressive stress (-1.0 MPa) and the compressive stress (-1.5 MPa) occurring due to fixed thermal

TABLE 1 Material Parameters

Young's Modulus of Solid Phase(*MPa*)	1.5×10^4
Volumetric Young's Modulus of Liquid Phase(*MPa*)	2.2×10^3
Effective Stress due to Volumetric Contraction(*MPa*)	−1.0
Pore Pressure due to Volumetric Contraction(*MPa*)	−1.0
Coefficient of Thermal Expansion(/℃)	1.0×10^{-5}
Changing of Temperature(℃)	±10.0

expansion. In the liquid phase, deformation due to the initial stress state is contraction while the thermal deformation is expansion, i.e., the direction of these deformations are apposite and hence a negative (tension) pore water pressure of -0.78 MPa occurred as the sum of the initial tensile stress (-1.0 MPa) and the compressive stress (0.22 MPa) occurring due to fixed thermal expansion. Here, the sign is defined as positive for tensile stress and compressive pressure. As the total stress is defined as the difference between effective stress and pore water pressure, the analytical result in which the initial stress state and pore water pressure are in trounced is -1.72 MPa, a value -0.22 MPa greater than that obtained by conventional analysis (-1.5 MPa). On the other hand, as the concrete temperature falls, in the solid phase, the deformation of the initial stress state is expansion and the thermal deformation is contraction, so a effective tensile stress of 0.5 MPa arose as the sum of the initial compressive stress (-1.0 MPa) and the tensile stress (1.5 MPa) due to fixed thermal contraction. In the liquid phase, both the deformation of initial stress state and temperature are contractions, so a negative (tension) pore water pressure of -1.22 MPa occurred as the sum of the initial tensile stress (-1.0 MPa) and tensile stress (-0.22 MPa) due to fixed thermal contraction. The total stress is a value of 1.72 MPa, a value 0.22 MPa greater than that of the conventional analysis (1.5 MPa). These results show that thermal stress with age is higher than that given by conventional analysis when the initial stress state and pore water pressure are introduced, as shown in Fig.12.

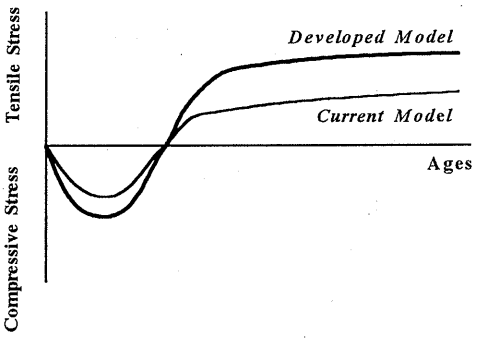

Fig. 12 Characteristics of Thermal Stress

Secondly, we estimate the effect of initial stress state and pore water presure on thermal stress behavior when the creep effect is considered. The examination was performed in the special state such that the initial stress was reduced to zero as a result of creep. That is, the difference between this analytical result and the conventional analysis is only the value of pore water pressure occurring due to thermal stress deformation. During the rise in concrete temperature, a positive (compression) pore water pressure occurs in our analysis due to the fixed thermal expansion of concrete. On the other hand, as the concrete temperature falls, a negative (tension) pore water pressure occurs due to the fixed thermal contraction of concrete. Therefore, as with the earlier results in which the creep effect was ignored, this analysis gives thermal stress with age that is larger than that given by conventional analysis, as shown in Fig.12. The fact that thermal cracking in actual concrete structures occur earlier than predicted by analysis, as has been reported, may be due in part to effect of initial stress state and pore water pressure.

These results for the simplest model, a one-dimensional thermal stress problem, indicate that the effects of initial stress state and pore water pressure must be introduced to analytically predict thermal stresses in detail.

5. PORE WATER PRESSURE IN EARLY-AGE CONCRETE

In the experimental study on pore water pressure, the experimental parameters were the loading age, pre-loading age, ratio of pre-loading stress to uni-axial compressive strength, and curing period in water. It should be noted that the main factor affecting pore water pressure and concrete stress characteristics was water content. A high pore water pressure occurs compared with concrete stress, and there is an inflection which indicates the existence of negative pore water pressure in the voids formed by hydration during a curing. In this section, an analytical estimation of pore water pressure occurring in concrete due to the application of an external load is performed, taking into account the initial stress state caused by hydration. The mechanism of water migration in concrete is discussed.

The disposal method of concrete specimens from concrete placing to the application of the external load is shown in Table.2. The specimen is removed from the form at the age of 1 day and pre-loading stress is applied at the age of 1, 3, and 5 days. The loading stress is then immediately released, and then the specimen is cured in water or air and finally the pore water pressure tests are performed at the age of 3 7 days, as shown in Table.2. Analysis was performed for all concrete specimen shown in Table.2. The meaning of the symbols and numbers of the specimen No. shown in Table.2 are illustrated belon taking Ⅲ1-0-90 as an example.

TABLE 2 Curing Method of Concrete Specimen and Pre-Loading Stress

Specimen	Disposal Method of Concrete Specimen	Degree of Damage(%)
Ⅲ 1-0-0	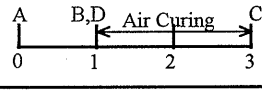	0
Ⅲ 1-0-60		60
Ⅲ 1-0-90		90
Ⅲ 1-2-0	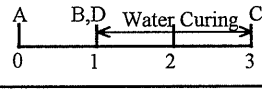	0
Ⅲ 1-2-60		60
Ⅲ 1-2-90		90
Ⅶ 3-2-0	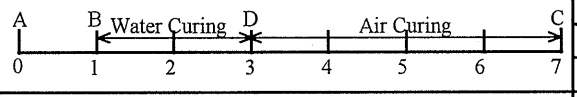	0
Ⅶ 3-2-60		60
Ⅶ 3-2-90		90
Ⅶ 3-4-0	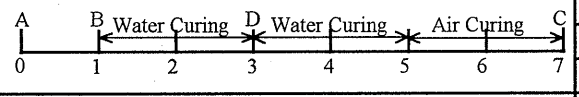	0
Ⅶ 3-4-60		60
Ⅶ 3-4-90		90
Ⅶ 3-6-0	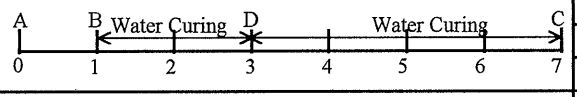	0
Ⅶ 3-6-60		60
Ⅶ 3-6-90		90
Ⅶ 5-4-0	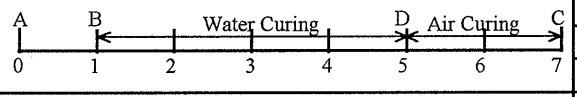	0
Ⅶ 5-4-60		60
Ⅶ 5-4-90		90
Ⅶ 5-5-0	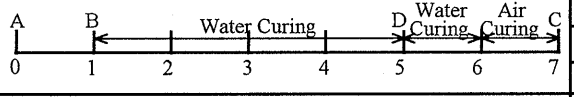	0
Ⅶ 5-5-60		60
Ⅶ 5-5-90		90
Ⅶ 5-6-0	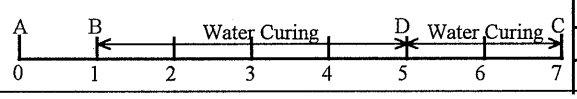	0
Ⅶ 5-6-60		60
Ⅶ 5-6-90		90

A: Placing B: Removal of Forms
C: Loading D: Pre-Loading Stress to Uni-Axial Compressive Strength

Ⅲ : loading age (day)
1 : age at which pre-loading stress is introduced (day)
0 : water curing period (day)
90 : ratio of pre-loading stress to uni-axial compressive strength (%)

In the following discussion, specimens Ⅲ1-0-0,60,90 and Ⅲ1-2-0,60,90 are defined as theⅢ1, series Ⅶ3-2-0,60,90 and Ⅶ3-6-0,60,90 as the Ⅶ3, series Ⅶ5-4-0,60,90 and Ⅶ5-6-0,60,90 as the Ⅶ5 series.

The method of applying the developed analytical model the concrete specimens with pre-loading stress (called "damage") is such that the damage parameter[7] with pre-loading stresses of 60,and 90% of the uni-axial compressive strength calculated by elasto-plastic analysis in the uni-axial compressive state and then the developed water migration analysis is performed using the obtained damage parameter as the initial value of concrete damage. The boundary conditions in the analysis are fixed of lateral displacement and pore water completely undrained. In the following discussion, the applicability of the developed model is discussed by comparing it with the experimental results and an analytical estimation of the pore water pressure occurring in concrete due to the application of an external load is performed. Then the mechanism of water migration in concrete is discussed.

5.1 Ⅲ1 Series

Figs.13, 14, 15 and 16 give the analytical and experimental results for specimen Ⅲ 1-2, where the loading age was 3 days and the specimen was cured in water after the application of pre-loading stress, and Ⅲ1-0, where the loading age was 3 days and the specimen is cured in air. Figs.13 and 15 show the relationship between total stress and total strain and, Figs.14 and 16 show the relationship between pore water pressure and total strain. In each figure, the analytical results shown with the solid, dotted and broken lines, while the experimental results are shown by circles, triangles, and squares for the pre-loading stresses 0, 60,and 90%, respectively. Further, the inflection point is shown by a white circle.

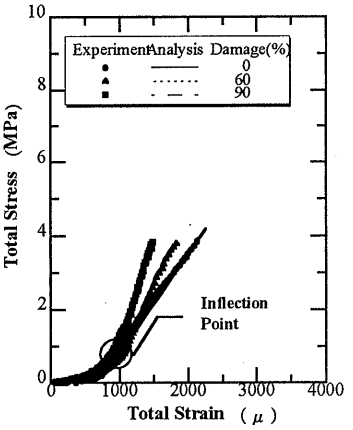

Fig. 13 Characteristics of Total Stress(Ⅲ 1-2 Specimens)

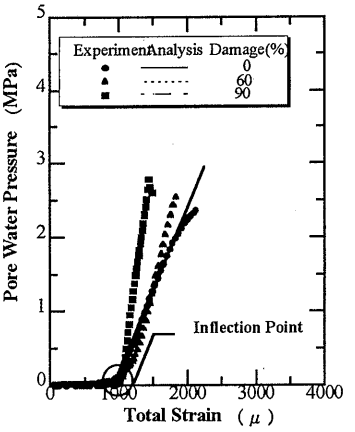

Fig. 14 Characteristics of Pore Water Pressure(Ⅲ 1-2 Specimens)

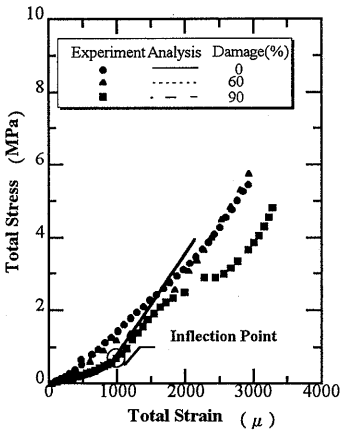

Fig. 15 Characteristics of Total Stress(Ⅲ 1-0 Specimens)

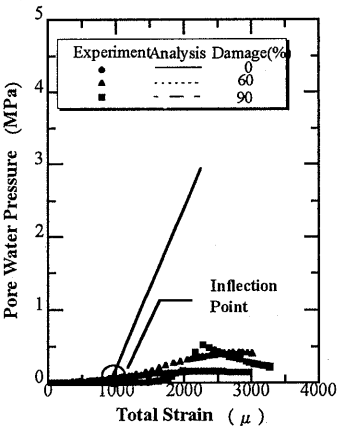

Fig. 16 Characteristics of Pore Water Pressure(Ⅲ 1-0Specimens)

As shown in Figs.13 and 14, the analytical results give good agreement with the experimental results except for the pre-loading stress of 90%. The analytical examination indicates that the concrete specimen becomes saturated with water at a strain corresponding to the inflection point due to the canceling out of the initial pore water pressure caused by hydration and the loading stress; the increase in pore water pressure is then linear. This behavior is caused by the phenomenon shown in Fig.17. The initial stress state before loading is such that a negative (tension) pore water pressure occurs in the liquid and gas phases as shown by the line of O-B and a compressive effective stress occurs in the solid phase shown by the line O-C. Applying the forced displacement O-D, the negative pore water pressure B-B and the compressive effective stress C-C are canceled out and the canceling of there initial stresses proceed with the increase of the forced strain and finally at the forced strain A, most of the initial stress occurring in the void and solid phases is canceled out at a point corresponding to inflection point A. After inflection point A, a sudden increase in total stress A-E and pore water pressure A-G occurs. Hence, it should be noted that the initial stress state caused by hydration has to be taken into consideration in estimating the water

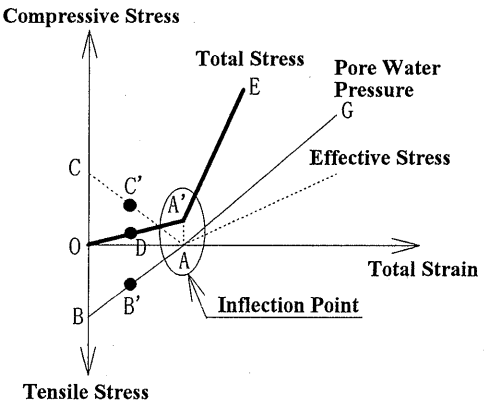

Fig. 17 Stress Path Considering Initial Stress State

migration problem. For the case of a pre-loading stress rate of 90%, the analytical gradients of total stress and pore water pressure were larger than the experimental values. The reason for this may be that the specific gravity and bulk modulus of the water are larger than the values used in the analysis due to cement particles mixing with the water.

On the other hand, in the case of Figs.15and 16, the analytical results of total stress and pore water pressure are quite different from the experimental results. The experimental results indicate the scarce of pore water pressure occur due to the extremely low water content of the concrete specimen, while the analytical results show a sudden and linear increase in pore water pressure after the initial pore water pressure reaches to zero due to an assumed saturation of the concrete. This analytical examination, indicates that it is impossible to apply the developed model to specimens which are not saturated with water at the initial pore water pressure of zero. However, it may be applied to unsaturated concrete it an adequate estimation of the decrease in bulk modulus resulting from mixing of liquid and gas can be made.

5.2 Ⅶ3 Series

Figures 18, 19, 20, and 21 give the analytical and experimental results for specimen Ⅶ3-6, which was loaded at 7 days and cured in water after the application of pre-loading stress and specimen Ⅶ3-2 which was loaded at 7 days and cured in air. Figures.18, 20 show the relationships between total stress and total strain, and Figs.19, 21 show the relationships between pore water pressure and total strain. In each figure, the analytical results are shown by solid, dotted, and broken lines, while the experimental results are shown with circles, triangles, and squares for the pre-loading stress rates 0, 60, and 90%, respectively. Further, the inflection point is shown by a white circle.

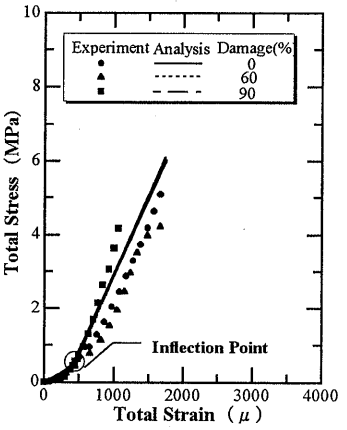

Fig. 18 Characteristics of Total Stress(Ⅶ 3-6 Specimens)

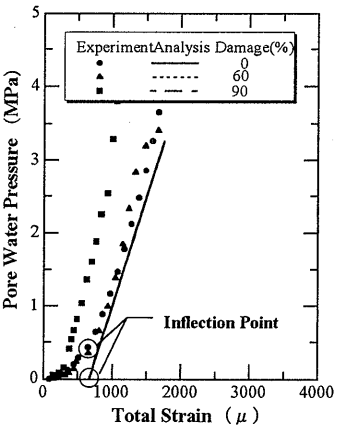

FIG.19 Characteristics of Pore Water Pressure(Ⅶ 3-6 Specimens)

The analytical results show a good agreement with the experimental results. The analytical total strain corresponding to the inflection point, shown by the white circle, is smaller than that of the Ⅲ1 series due to the relaxation of the initial stress state caused by creep during curing in water and due to the high stiffness of the concrete specimen.

On the other hand, in Figs.20 and 21, the difference between the analytical and experimental results is only the strain corresponding to the inflection point; the value obtained by analysis is smaller than the experimental value,

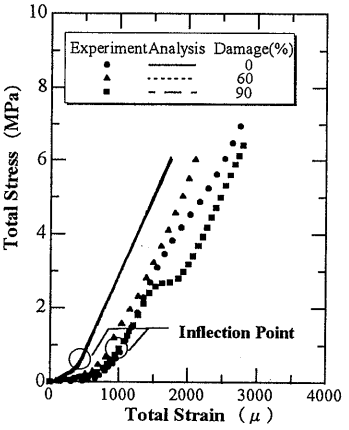

Fig. 20 Characteristics of Total Stress(Ⅶ 3-2 Specimens)

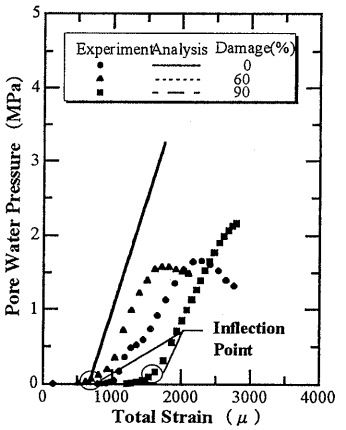

FIG.21 Characteristics of Pore Water Pressure(Ⅶ 3-2 Specimens)

and hence it seems that the developed model can be estimated the experiment due to the only detailed estimation of inflection point. From the analytical examination of a specimen assumed to be saturated, it seems that the initial stress of a specimen cured in water is less than that of one cured in air due to the relaxation of stress caused by the inflow of water to the specimen. This analytical examination will be more clarified due to the comparison with the experimental results for Ⅶ3-2 and Ⅶ3-6, i.e., the strain corresponding to the inflection point is smaller as the periods cured in water is longer. In this study, the relaxation of initial stress due to the inflow of water to the concrete specimen is treated as a creep phenomenon. Thus, the discrepancy between analytical and experimental results arises due to the very little relaxation or creep caused by long term curing in air in the case of experimental results for Ⅶ3-2.

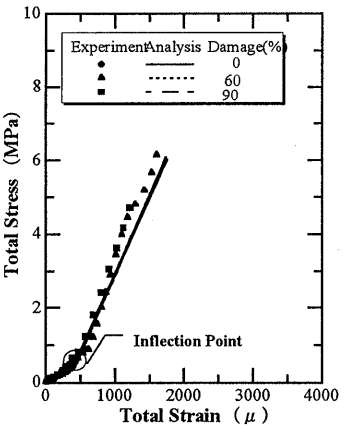

Fig. 22 Characteristics of Total Stress(Ⅶ 5-4 Specimens)

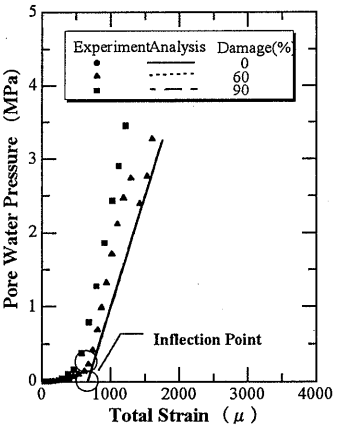

FIG.23 Characteristics of Pore Water Pressure(Ⅶ 5-4 Specimens)

5.3 Series of Ⅶ5

Figures.22, 23, 24, and 25 show the analytical and experimental results for specimen Ⅶ5-4, which was loaded at 7 days and in cured in air after application of the pre-loading stress, and Ⅶ5-6, which was loaded at 7 days and cured in water. Figures.22 and 24 show the relationships between total stress and total strain, while Figs.23 and 25 show the relationships between pore water pressure and total strain. In each figure, the analytical results are shown by solid, dotted, and broken lines, while the experimental results are shown by circles, triangles and squares for pre-loading stress ratios of 0, 60, and 90%, respectively. Further, the inflection point is shown by a white circle.

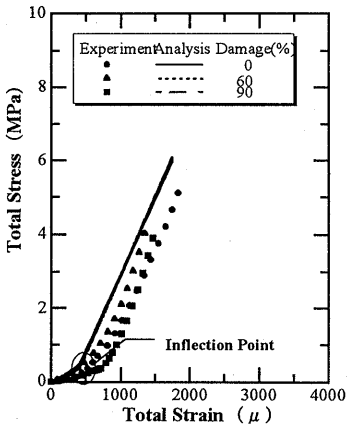

Fig. 24 Characteristics of Total Stress(Ⅶ 5-6 Specimens)

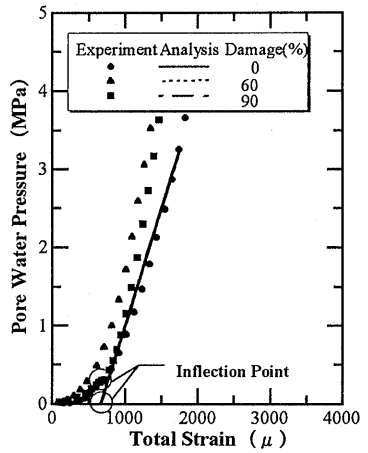

FIG.25 Characteristics of Pore Water Pressure(Ⅶ 5-6 Specimens)

As Figs.22～25, make clear the analytical results show good agreement with the experimental results on the whole. The analytical examination indicates seems that the concrete specimen becomes saturated with water at the inflection point, i.e., when the initial stress takes a value of zero due to the inflow of water to the concrete specimen caused by curing in water during the dominant hydration process. As with the Ⅶ3 series, the total strain corresponding to the inflection point is smaller and hence water migration will occurs at a lower strain level than in the specimen Ⅲ1 series.

All of these results demonstrate the applicability of the developed model to specimens which are cured in water during the dominant hydration process, with water migration taking place when the initial stress takes a value of almost zero, i.e., at the inflection point. Further, they demonstrate that in estimating the water migration problem, the initial stress state caused by hydration has to be taken into consideration.

6. ANALYTICAL ESTIMATION FOR EFFECT OF PORE WATER PRESSURE ON MECHANICAL CHARACTERISTICS OF CONCRETE

In the above section, it was confirmed that the developed model is applicable to specimens cured in water during the dominant hydration process.

In this section, an analytical consideration of the mechanism by which pore water pressure affects concrete strength is carried at by comparing concrete specimens which are assumed to be completely saturated and completely non-saturated. The analysis is carried out at the age of 3 days with the same boundary conditions as used previously. Analysis of the unsaturated specimen is carried out by taking the bulk modulus of the liquid and gas phases to be almost zero.

Figures.26 and 27 show the analytical results for saturated and unsaturated specimens; Fig.26 is the relationship between compressive total stress and total strain and Fig.27 is the relationship between positive (compression) pore water pressure and total strain. In each figure, the analytical results for the saturated and unsaturated specimens are shown with solid and dotted lines, respectively.

As shown in Figs.26 and 27, the effective stress of the unsaturated concrete specimen is equal to the total stress since there is no pore water pressure, and hence the effective stress of the saturated specimen is the same as the total or effective stress of the unsaturated concrete specimen. That is, the total stress of the saturated specimen is higher of pore water pressure compared with that of the unsaturated specimen if the stress and pressure are compressive according to Eq.(17). On the other hand, if the stress is compressive and pressure is tensile, the total stress of the saturated specimen is smaller of pore water pressure compared with that of the unsaturated concrete specimen. These stress properties are illustrated in Fig.28, which is the stress path and stress state from step (n) to step (n+1) in the $I_1 - \sqrt{J_2}$ plane. Namely, it seems that an increase in concrete strength of the saturated specimen occurs as compared with the unsaturated specimen if the stress and pressure are compressive. On the other hand, it seems that a decrease in strength of the saturated specimen occurs if the stress is compressive and pressure is tensile due to plastic volumetric expansion and shear deformation, such as in tri-axial compressive tests with constant lateral pressure.

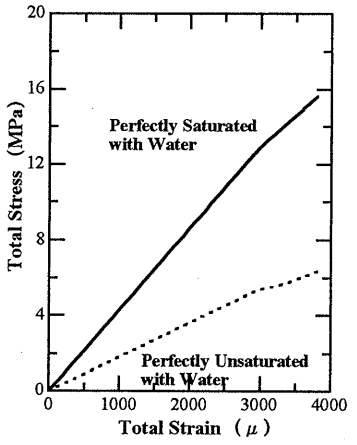

Fig. 26 Effect of Degree of Saturation with Water on Total Stress

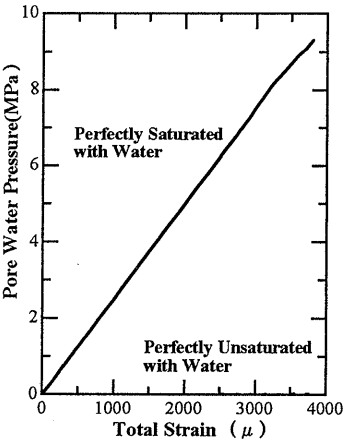

Fig. 27 Effect of Degree of Saturation with Water on Pore Water Pressure

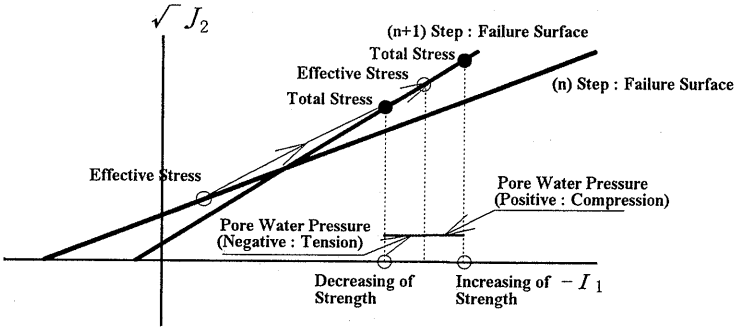

Fig. 28 Effective and Total Stress Path on Meridian Plane (Drucker-Prager Type)

Conclusions

In this study, an analytical theory of water migration applicable to porous permeable materials such as concrete and rock has been developed and an analytical examination of pore water pressure occurring in concrete due to external loading was carried out. Further, an analytical examination of the mechanism for the effects of pore water pressure on mechanical characteristics was carried at. The study has to the following conclusions:

(1) The initial stress state caused by hydration has to be taken into consideration in estimating the water migration problem.
(2) By considering volumetric contraction due to hydration in the developed model, the initial stress state can be estimated quantitatively
(3) The initial stress state and pore water pressure have a great influence on the thermal stress problem.
(4) The applicability of the developed model to water migration in concrete can be confirmed for concrete specimens cured in water.
(5) The compressive strength of a saturated concrete specimen with a fixed lateral displacement is larger than that of an unsaturated concrete specimen.

Notations

Q_{in}	:	inflow rate
Q_{out}	:	outflow rate
ΔV	:	accumulation rate
v_i	:	flow velocity of pore water
σ_{ij}	:	total stress
σ'_{ij}	:	effective stress
p	:	pore water pressure
m_{ij}	:	$[1 \ 1 \ 1 \ 0 \ 0 \ 0]^T$
G	:	Gibb s Free Energy
k_{ij}	:	permeability matrix
z	:	potential head
γ_w	:	specific weight of water
ρ_w	:	density of liquid phase
S_w	:	degree of saturation with liquid phase
ε_V	:	volumetric strain
t	:	time
ε_{ij}	:	total strain
ξ	:	porosity which depends on the rate of hydration of cement
D^{ep}_{Sijkl}	:	elasto-plastic stiffness matrix of solid phase
K_f	:	bulk modulus of liquid and gas phase
μ	:	coefficient of thermal expansion of liquid and gas phase
T	:	concrete temperature
ε^{cr}_{ij}	:	creep strain
η	:	rate of gel pore volume formed by the hydration to the initial cement volume
γ_p	:	water cement ratio of complete hydration
C_H	:	hydrated cement weight per unit cement volume
V	:	volume of concrete per unit controlled volume
V_A	:	volume of aggregate per unit controlled volume

V_C : volume of cement paste per unit controlled volume
C : initial cement weight
W : initial water weight
k_0, n_0 : material parameter denoted the hydration rate
q : spring flow from the unit controlled volume
$\{\varepsilon\}$: incremental total strain
$\{\overline{u}\}$: nodal displacement
$\{\overline{p}\}$: nodal pore water pressure
N : shape function for displacement
$\overline{N}$: shape function for pore water pressure, etc.
Ω : volume of concrete body
Γ : surface area of concrete body
$d\sigma'_{ij}$: incremental effective stress
$d\sigma_{ij}$: incremental total stress
$d\varepsilon^t_{ij}$: incremental total strain
$d\varepsilon^{pr}_{ij}$: incremental pore water pressure strain
$d\varepsilon^{hyd}_{ij}$: incremental volumetric contraction strain
$d\varepsilon^{cr}_{ij}$: incremental creep strain
$d\varepsilon^t_{Aij}$: incremental total strain of aggregate
$d\varepsilon^t_{Cij}$: incremental total strain of cement paste
$d\varepsilon^{pr}_{Aij}$: incremental pore water pressure strain of aggregate
$d\varepsilon^{pr}_{Cij}$: incremental pore water pressure strain of cement paste
t_0 : age by day
t'_0 : loading age by day
a_0, b_0, c_0 : material parameter for creep strain
$d\overline{T}$: incremental concrete temperature
$d\overline{f}_i$: incremental external load
B_i : strain and displacement relation
α : coefficient of thermal expansion of solid phase
b_i : body force
t_i : surface force

References

[1] Oshita, H., and Tanabe, T. : Experimental Study on Measuring Pore Water Pressure Occurring in Concrete and Its Effects, *Pro. of JSCE,* No.514 / V-27, May, pp.75-84, 1995 (in Japanese)

[2] Bazant, Z. P., and Najjar, L. : Nonlinear Water Diffusion in Nonsaturated Concrete, *Materiaux et Constructions,* Vol.5, No.25, pp.3-20, 1972

[3] Kawasumi, M., Kasahara K., and Kuriyama. T. : Creep Property of Concrete under High Temperature (Effect of Thermal Property on Hydration Reaction of Cement), *Report of Central Research Institute*, No.381025, 1981 (in Japanese)

[4] Czernin.W : Cement Chemistry for Construction Engineering, 1969

[5] Murata, J. : Studies on the Permeability of Concrete, *Trans. Of JSCE*, No.77, Nov., pp.69-103, 1961

[6] Powers, T. C., Copeland, L. E., Hayes, J. C., and Mann, H. M. : Permeability of portland Cement Paste, *ACI Journal*, No.51-14, Nov., pp.285-298, 1954
[7] Wu, Z. S., and Tanabe, T. : A Hardening-softening Model of Concrete Subjected to Compressive Loading ,*Journal of Structural Engineering, Architectual Institute of Japan*, Vol.36B, pp.153-162, 1990.
[8] Inoue, T. : Study on the Deformational Behavior of Concrete at Early Ages, Master's Thesis at Nagoya University, 1990 (in Japanese)
[9] Tazawa, E., and Miyazawa, S.: Autogeneous Shrinkage of Concrete and its Importance in Concrete Technology, *Proc. of the Fifth International RILEM Symposium*, pp.159-168, 1993